

ON THE APPLICATION OF WALL BOILING MODELS TO PREDICTION OF SUBCOOLED FLOW BOILING USING EAGLE CODE

N. H. Hoang, I. C. Chu, D. J. Euh, and C. H. Song*

Korea University of Science and Technology / Korea Atomic Energy Research Institute

Daedeok-daero 989-111, Yuseong-gu, Daejeon, Korea

hnhien@kaeri.re.kr; chuic@kaeri.re.kr; djeuh@kaeri.re.kr; chsong@kaeri.re.kr

ABSTRACT

Mechanistic modeling of the subcooled flow boiling requires a combination of so-called wall boiling models, i.e. heat flux partitioning models and models/correlations of nucleation site density, bubble departure diameter and bubble departure frequency, to compute the near-wall boiling heat transfer. Despite a large number of the wall boiling models have been introduced to support this approach, the applicability of these models to the computation of the near-wall boiling heat transfer is still limited and debatable. In this study, we carried out a detailed evaluation of the existing wall boiling models that have been used widely. The models were firstly reviewed and assessed against the selected available experimental data. The combinations of the models that showed good predictability were then evaluated via the CFD simulation of the DEBORA experiment, which investigated the forced convective subcooled boiling of refrigerant R-12 in a vertical channel. The simulation was performed with EAGLE code, an in-house CFD code for multi-dimensional analyses of the subcooled flow boiling. It is found that the combinations of different wall boiling models provided a good prediction of the boiling flow characteristics, i.e. void fraction, interfacial area concentration and Sauter mean diameter, but showed large differences in the divided heat flow rates, nucleation site density, bubble departure diameter, bubble departure frequency and wall temperature. These parameters seem to be self-adjusted to satisfy the energy balance requirement rather than reflecting their actual values. It is possibly due to the fact that some significant mechanisms by which the total heat flux is partitioned are still not accounted for.

KEYWORDS

Subcooled flow boiling, Near-wall heat transfer, Wall boiling models, DEBORA, EAGLE code

1. INTRODUCTION

Subcooled flow boiling is of great importance to many industrial applications, e.g., nuclear reactors and fossil boilers, in which large heat transfer rate is required. It directly concerns the performance and safety of the relevant systems. Consequently, the modeling of the subcooled flow boiling is very essential to the design optimization and safe operation of the systems. Nevertheless, the attempts to predict the subcooled flow boiling have had limited success due a large part to the complexity of the boiling heat transfer in the vicinity of the heated wall. The sub-processes, i.e. heat transfer mechanisms, bubble dynamics, bubble nucleation and thermal response of the heated surface, involved in the near-wall boiling heat transfer are very complicated and challenging to both the experimental measurement and mathematical modeling [1]. In order to succeed in the modeling of the subcooled flow boiling, satisfactory models/correlations characterizing the sub-processes have been required.

In common, the near-wall boiling heat transfer has been described by a combination of a reasonable heat flux partitioning model with models/correlations of nucleation site density, bubble departure diameter and bubble departure frequency [1-6]. A large number of the models/correlations supporting this approach have been introduced [6]. Nevertheless, the applicability of the models/correlations is relatively limited and debatable in practice. Tu and Yeoh [2], Krepper and Rzehak [3], Yun et al. [5], Cheung et al. [6], etc., obtained good predictions of subcooled boiling flows by means of CFD simulation. They used Kural and Podowski's model of the heat flux partitioning in combination with different models/ correlations of the nucleation site density, bubble departure diameter and bubble departure frequency. The predicted boiling flow characteristics, such as void fraction, Sauter mean diameter and interfacial area concentration (IAC) agreed well with the experimental data. However, a single combination of the wall boiling models was unable to provide satisfactory predictions covering entire axial and local flow conditions. Different simulations might require different model combinations. Furthermore, the near-wall boiling heat transfer characteristics, i.e. the nucleation site density, bubble departure diameter and bubble departure frequency, given by such model combinations can be very different to each other.

A practical need concerning the modeling of the subcooled flow boiling is to re-evaluate in detail the models and correlations that have been used widely in computations of the near-wall boiling heat transfer. To aim for this purpose, this study carried out a detailed review and assessment of the models and correlations based on published experimental data. And then the implementation of the model and correlations into a CFD code, namely EAGLE, was presented. Finally, an assessment of the models and correlations in different combinations against the DEBORA experiment, which investigated the forced convective subcooled boiling of refrigerant R-12 in a vertical channel, was performed. The boiling flow characteristics as well as the physical linkage between the models/correlations were revealed via this assessment.

2. WALL BOILING MODELS

In the framework of the CFD modeling of the subcooled flow boiling, the wall boiling models, i.e. the models/correlations of the heat flux partitioning, nucleation site density, bubble departure diameter and bubble departure frequency, occupy a very important position. They characterize the hydrodynamics and heat transfer near the heated surface. The boiling characteristics like wall temperature, nucleation site density, rate of phase change, etc. are calculated by the combination of these models and inputted into the two-phase flow governing equations as the boundary conditions. Owing to the vital role, a great number of the models/correlations of this type have been proposed. The following sections present the detailed evaluation of the models.

2.1. Heat Flux Partitioning Model

One taking the central role in the computation of the near-wall boiling heat transfer is the heat flux partitioning model. This model provides information regarding how the wall heat flux is partitioned between the liquid and vapor phases near the heated surface. Numerous empirical correlations and mechanistic models for the wall heat flux partitioning have been proposed on the base of related heat transfer mechanisms [7]. In general, the empirical correlations were formulated by superimposing the single-phase forced convection component onto the component induced by vapor bubbles presented on the heated surface. The component related to the bubbles can be divided further into the heat flux caused by the evaporation at the bubble base and the heat flux induced by bubble agitation in the thermal boundary layer. The heat fluxes were formulated empirically based on particular experiments, hence limitation in the application range. To overcome the limitation, many researches have introduced the mechanistic models. In these models the mechanisms by which the heat is taken away from the heated surface were clarified clearly, and the heat flux components were modeled mechanistically via related physical parameters [7]. Therefore, the mechanistic model will be considered further here.

Recent CFD simulations of the subcooled flow boiling have employed Kural and Podowski's model for dividing the heat flux supplied from the heated surface [2–7]. In this model, total heat flux (q_w) is divided into the three components: single phase ($q_{1\phi}$), transient conduction (q_q) and evaporation (q_e).

$$q_w = q_e + q_q + q_{1\phi} \quad (1)$$

where

$$q_e = N_a f \left(\frac{\pi}{6} d_b^3 \right) \rho_v h_{fg} \quad (2)$$

$$q_q = \left(\frac{2}{\sqrt{\pi}} \sqrt{t_w k_l \rho_l C_{pl} f_b} \right) A_q (T_w - T_l) \quad (3)$$

$$q_{1\phi} = h_c (1 - A_q) (T_w - T_l) \quad (4)$$

$$A_q = N_a \left(K \frac{\pi d_b^2}{4} \right) \quad (5)$$

In order to employ this model, models/correlations of the nucleation site density (N_a), bubble departure diameter (d_b), bubble departure frequency (f_b) and waiting time (t_w) are required.

Although Kural and Podowski's model have been used widely in CFD simulations, it exits three important aspects needed to be considered deeply. They are the overlap of areas influenced by bubbles, heat transfer enhancement by micro-convection and bubble sliding and merger, as shown in Fig. (1).

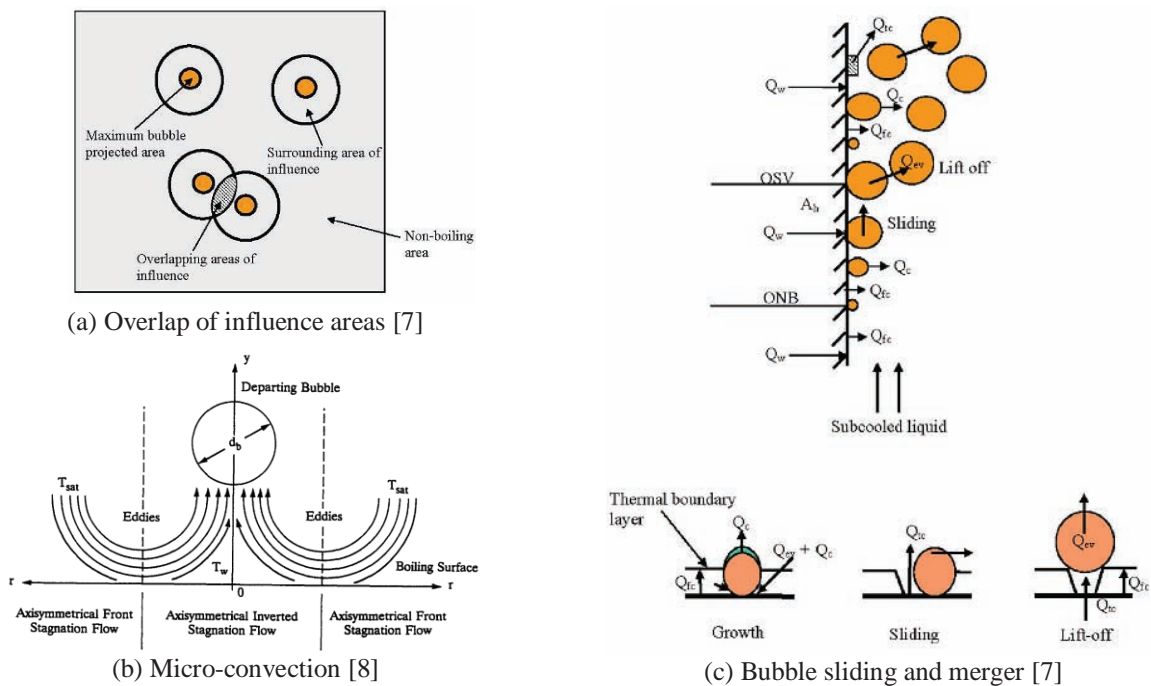


Figure 1. Heat Flux Partitioning Models.

The empirical constant K in Eq. (5) accounts for the fraction of heated surface area influenced by the bubbles. It takes a value of 4. This value represents the heated surface covered by separate bubbles exiting under low and middle heat fluxes. However, when more nucleation sites are activated with increasing the heat flux, the nearby influential areas are possibly overlapped (Fig. 1a) and the factor K should take a different value rather than 4. This causes a significant change in the fraction of the heat transfer components. Del Valle and Kenning [9] quantified the degree of the overlap by multiplying the nominal boiling fraction by a reduced factor X . Both the K and X factors, however, are not known a priori. They were just tabulated according to several wall heat flux values. For widening the application of Kural and Podowski's model, a mechanistic model/empirical correlation accounting for the overlap is required.

The second aspect is the heat transfer enhancement due to the micro-convection happened in the region of the heated surface behind the wake of departing bubbles (Fig. 1b). The quenching component of Kural and Podowski's model given by Eq. (3) is actually the pure transient conduction heat flux obtained by Mikic and Rohsenow [8]. Nevertheless, Haider and Webb [9] showed that Mikic and Rohsenow's model is severely underestimated the Nakayama et al. and Chien's boiling data. According to their finding, the micro-convection formed in the region of the heated surface behind departing bubbles enhances the removal of heat from the heated surface and the heat transfer enhancement was accounted for by multiplying the Mikic and Rohsenow's quenching heat flux by a factor as follows:

$$q_{q,mc} = q_q \times \left[1 + \left(0.66\pi c \cdot \text{Pr}^{-1/6} \right)^x \right]^{1/x} \quad (6)$$

Haider and Webb [9] gave different values of the empirical constants c and x for different working fluids. This model will be evaluated in this study. However, the given values of the empirical constants might not appropriate for most cases.

The last aspect is the bubble sliding and bubble merger as raised by Basu et al. [7]. Vapor bubbles generally experience a sliding while still growing. After sliding the bubbles can lift off the surface and enter the subcooled liquid if they do not encounter other bubbles (Fig. 1c). However, a significant increase in the number of active nucleation sites especially in the downstream of OSV (Onset of Significant Void) leads to reduce the distance between the bubbles. The possibility of the bubble merger consequently increases. Both the bubble sliding and bubble merger affect the heat transfer at the heated surface. Basu et al. [7] suggested a model quantifying the contribution of both these phenomena to the total heat removal at the surface. This model is however quite complicated. The determination of the spacing between the nucleation sites, the sliding distance from the departure to lift-off and the conditions by which the bubbles slide or merge is not easy and uncertain. An easier way is to use Kural and Podowski's model with estimated multiplying factors quantifying these phenomena.

2.2. Nucleation Site Density

The number of nucleation sites activated on a unit area of the heated surface when the surface temperature exceeds the saturation liquid temperature at the local pressure is a governing parameter of the near-wall boiling heat transfer. The dynamic of vapor bubbles formed at these sites and of surrounding liquid are mutually changed with the variation of the nucleation site density, hence varying the heat flux division. Nevertheless, the determination of the nucleation site density is rather difficult especially at high heat flux conditions. More nucleation sites become activated leading to significant coalescence of the bubbles and overlap of the influential areas. This makes the discrimination and count of the nucleation sites in experimental measurements very difficult. In addition, the formation of the nucleation sites highly depend on many factors, i.e., the surface roughness, geometry of microscopic scratches and pits on the heated surface, fluid wettability, purity and surface material, which are difficult to control [6,10]. Thus, very few

correlations of the nucleation site density have a wide applicability. In general, the nucleation site density can be expressed as a function of the wall superheat or minimum cavity size R_c as given in Eq. 7.

$$N_a = \begin{cases} N_{a,0} (T_w - T_{sat})^n \\ N_a (R_c) \end{cases} \quad (7)$$

Most existing correlations of the nucleation site density can be recast following Eq. (7), as shown in Table I. It is observed readily that the correlations expressed in the first form are very different in the multiplying factor $N_{a,0}$ and exponent n . The multiplying factor is a constant in Lemmert and Chawla's correlation, a function of thermo-physical properties of liquid and surface material in Benjamin and Balakrishnan's correlation, or a function of the contact angle θ in Basu et al.'s correlation. Similarly, the exponent n varies significantly from 1.805 in Lemmert and Chawla's correlation to 5.3 in Basu et al.'s correlation. Hibiki and Ishii [11] suggested that the exponent n varies with the critical cavity size, which is a function of the wall superheat. This suggests expressing the nucleation site density in the second form. Nevertheless, the correlations given in the second form also show a difference in the effect of the critical cavity size on the nucleation site density. They indicate that the nucleation site density is proportional to $R_c^{-4.4}$, R_c^{-6} and e^{-R_c} , as seen in Table I.

Table I. Nucleation Site Density Models

Model	$N_a = N_{a,0} (T_w - T_{sat})^n$		Application
	$N_{a,0}$	n	
Lemmert and Chawla [6]	$210^{1.805}$	1.805	Pool boiling of saturated water
Benjamin and Balakrishnan [6]	$218.8 \text{Pr}^{1.63} \left(\frac{1}{\gamma} \right) \Theta^{-0.4}$	3	Pool boiling of saturated liquids (water, R-10) at low-to-moderate heat flux, $1.7 < Pr < 5$, $4.7 < \gamma < 93$, $0.02 < Ra \text{ (mm)} < 1.17$, $5 < \Delta T_{sat} \text{ (K)} < 25$, $10 < \sigma \text{ (N/m)} < 59$
Basu et al. [11]	$3.4 \times 10^4 (1 - \cos \theta)$ (for $\Delta T_{ONB} < \Delta T_{sup} < 15$)	2	Forced convective boiling of subcooled water at atmospheric pressure, $124 < G \text{ (kg/m}^2\text{s)} < 886$, $6.6 < \Delta T_{sub,in} \text{ (K)} < 52.5$, $2.5 < q_w \text{ (W/cm}^2) < 96$, $30^\circ < \theta < 90^\circ$
	$0.34(1 - \cos \theta)$ (for $\Delta T_{sup} \geq 15$)	5.3	
	$N_a = N_a (R_c (T_w))$		
Kocamustafaogullary and Ishii [11]	$f(\rho^*) (2R_c)^{-4.4} d_{bF}^{2.2}$		Pool/forced convective boiling of water, $0.1 \leq P \text{ (MPa)} \leq 19.8$
Wang and Dhir [11]	$7.81 \times 10^{-29} (1 - \cos \theta) R_c^{-6}$		Pool boiling of saturated water at atmospheric pressure, $18^\circ \leq \theta \leq 90^\circ$, $R_c < 2.9 \mu\text{m}$
Yang and Kim [11]	$\overline{N}_a \int_0^\theta \frac{1}{2\pi s} \exp \left[-\frac{1}{2} \left(\frac{\beta - \overline{\beta}}{s} \right)^2 \right] ds \cdot e^{-\lambda R_c}$		Depending on boiling surface (material, finish) and the half of cone angle β
Hibiki and Ishii [11]	$\overline{N}_a \left[1 - \exp \left(-\frac{\theta^2}{8\mu^2} \right) \right] \left\{ \exp \left[f(\rho^+) \frac{\lambda'}{R_c} \right] \right\}$		Pool/forced convective boiling of water, freons, ethalnoI, $0 \leq G \leq 886$, $0.101 \leq P \leq 19.8$, $5^\circ \leq \theta \leq 90^\circ$, $10^4 \leq N_a \leq 1.51 \times 10^{10}$

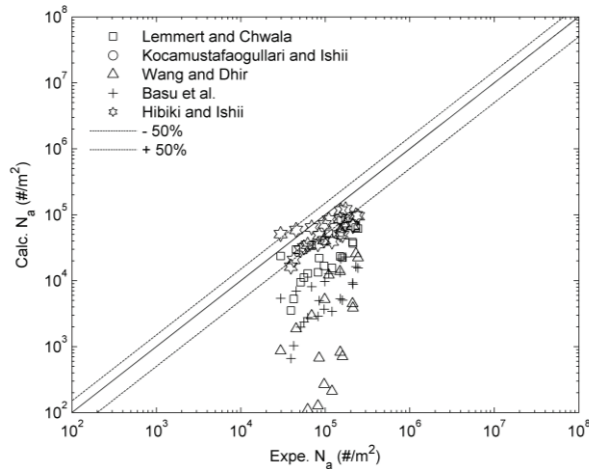


Figure 2. Chien et al.'s data.

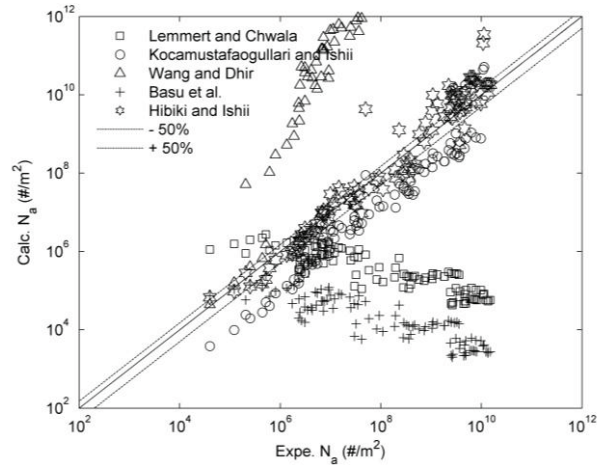


Figure 3. Borhishanskii et al.'s data.

In the present study, an assessment of the correlations against two published experimental data, i.e. Chien et al. [10] and Borhishanskii et al.'s [11] data, was performed. Owing to the difference in the effect of the related parameters, a significant difference in the estimated nucleation site density is anticipated. As shown in Fig. 2, the correlations are almost significantly underestimated Chien et al.'s data, which were measured for the subcooled pool boiling of refrigerant R-123 at the atmospheric pressure. Only Lemmert-Chawla and Hibiki-Ishii's correlations show a good match with this experimental data. Similarly, an interesting finding was revealed in the assessment against Borhishanskii et al.'s data, which were measured for the subcooled flow boiling of water at high pressures. As seen in Fig. 3, only Kocamustafaogullari-Ishii and Hibiki-Ishii's correlations agree with the experimental data. The others are either severely underestimated or overestimated. Especially Lemmert-Chawla and Basu et al.'s correlations, which show N_a proportional to $(T_w - T_{sat})^n$, are opposite to the experimental data. Meanwhile, Wang and Dhir's correlation that show N_a proportional to R_c^{-6} is remarkably overestimated.

In fact, Lemmert and Chawla's correlation seems valid for pool boiling at low pressures while Kocamustafaogullari and Ishii's correlation was developed for high pressures [11]. These two correlations therefore agree only with one of these experimental data. On the other hand, Hibiki and Ishii's correlation was developed physically based on Yang and Kim's approach [11]. Hibiki and Ishii introduced functions of the number of the cavity in terms of the cavity radius and half of cone angle, which characterize the heated surface, to estimate the active nucleation site density. Hence, the agreement of Hibiki and Ishii's correlation with both these experimental data is expected.

2.3. Bubble Departure Diameter

The bubble departure diameter is a primary bubble dynamic characteristic. This refers to the bubble diameter at departure. In fact, the bubble diameter at the lift-off instant (or bubble lift-off diameter) and maximum bubble diameter have been employed for the same purpose. Most existing correlations of the bubble departure and lift-off diameters were formulated based on the balance of forces acting on the bubble at the departure or lift-off instant. Fritz, Cole, Cole and Rohsenow, and Kocamustafaogullari and Ishii's correlations listed in Table II belong to this group. Other complicated correlations of the bubble lift-off diameter, which were developed based on the similar approach but given in an implicit form, like Klausner et al. [12] and Situ et al.'s [13] correlations are also available in the literature. Yun et al. [5] succeeded in using Klausner et al.'s correlation for the simulation of DEBORA experiment. However, Van Helden et al. [14] claimed that such force-balance models exist weak points. They contain unknown

parameters and the departure/lift-off criterion is not known exactly. Alternatively, several studies attempted to model the maximum bubble diameter by maximizing the bubble growth diameter derived from the energy balance equation at the bubble. Unal's correlation shown in Table II is one in this group. Tu and Yeoh [2] adopted successfully Unal's correlation for the modeling of low-pressure subcooled boiling flows. Besides these mechanistic approaches, the bubble departure diameter, bubble lift-off diameter and maximum bubble diameter can be predicted by means of empirical correlations, e.g. Tolubinsky and Kostanchuk's correlation, which are formed by correlating experimental data following a specific form [15,16]. Such correlations however often lack generality and are limited in applications.

In general, the correlations of the bubble departure diameter, bubble lift-off diameter and maximum bubble diameter used widely in the CFD simulation of the subcooled flow boiling can be rewritten in the following form.

$$d_b = d_{b,0} (T_w - T_{sat})^m \quad (8)$$

As shown in Table II, the exponent m takes values of 0, 1 or 2, and the multiplying factor $d_{b,0}$ is a function of the thermal properties of the fluid and/or surface material, contact angle, subcooling temperature and/or pressure. The thermal properties are in turn a function of the liquid temperature and pressure. Consequently, for a certain liquid temperature and pressure the bubble diameter predicted by the correlations which do not include the effect of the wall superheat is nearly constant. This is shown clearly via the assessment of these correlations against the experimental data reported by Situ et al. [13], Prodanovic et al [15] and Chu's [16]. As seen in Fig. 4, the bubble departure diameter predicted by Fritz, Cole-Rohsenow, Toulubinsky-Kostanchuk and Kacaomustafaogullari-Ishii's correlations is almost unchanged, just in different ranges. On the other hand, the correlations like Cole, Unal and Situ et al.'s correlations showed the evident variation of the bubble diameter with the wall superheat. Among all these correlations, Unal's correlation showed the best agreement with all the experimental data while Cole-Rohsenow and Toulubinsky-Kostanchuk's correlations gave the bubble diameter most close to the mean of the experimental data.

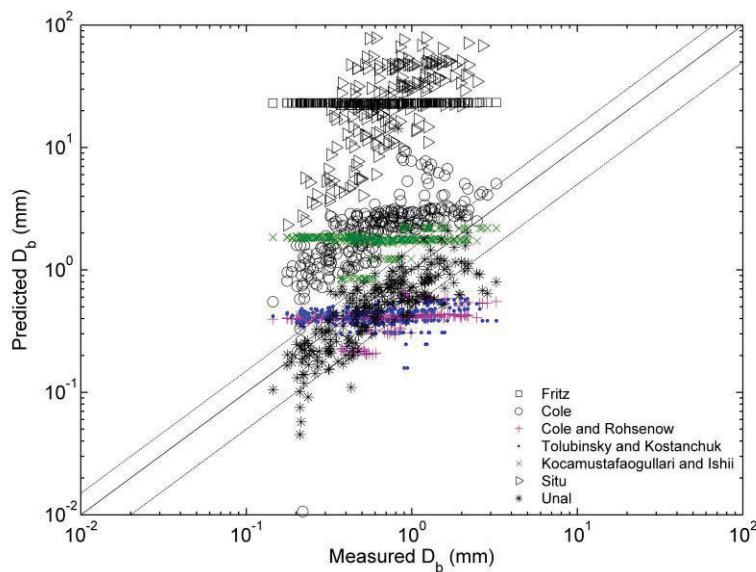


Figure 4. Bubble Departure Diameter

Table II. Bubble Departure Diameter Models [6,13,16]

Model	$d_b = d_{b,0} (T_w - T_{sat})^m$		Application
	$d_{b,0}$	m	
Fritz	$0.208\theta\sqrt{\sigma/g\Delta\rho}$	0	Pool boiling, low pressure
Cole	$4 \times 10^{-2} \sqrt{\frac{\sigma}{g\Delta\rho} \frac{\rho_l C_{pl}}{\rho_v h_{fg}}}$	1	Nucleate pool boiling at sub-atmospheric pressure
Cole and Rohsenow	$C_{fs} \left(\frac{\sigma}{g\Delta\rho} \right)^{1/2} \left(\frac{\rho_l C_{pl} T_{sat}}{\rho_v h_{fg}} \right)^{5/4}$	0	Pool boiling over a restricted pressure range
Tolubinsky-Kostanchuk	$\min \left[d_{ref} \exp(-\Delta T_{sub}/\Delta T_{ref}), 0.0014 \right]$	0	$d_{ref} = 0.6 \text{ mm}, \Delta T_{ref} = 45$
Unal	$\frac{1.21 \times 10^{-5} P^{0.709}}{\rho_v h_{fg}} \left(\frac{k_w \rho_w C_{pw}}{\pi b \Phi} \right)^{1/2}$	1	Subcooled flow boiling of water, $0.1 < P(\text{MPa}) < 17.7$
Kocamustafaogullari and Ishii	$2.64 \times 10^{-5} \theta (\Delta\rho/\rho_v)^{0.9} (\sigma/g\Delta\rho)^{0.5}$	0	Water, $0.67 < P(\text{MPa}) < 14.2$
Situ et al.	$\frac{4\sqrt{22/3}b^2}{\pi} \left(S \cdot \frac{\rho_f C_{pf}}{\rho_f h_{fg}} \right)^2 \frac{v_f}{\sqrt{C_1 u_r Pr_f}}$	2	Subcooled flow boiling of water at low pressure

2.4. Bubble Departure Frequency

The bubble departure frequency is physically defined as the inverse of growth time plus waiting time. The correlations/models developed based on this definition, for example Stephan’s correlation and Podowski et al.’s model [6], usually have complicated functional forms and are difficult for implementation into computational codes. For seeking simplicity, the waiting time has been assumed to be negligible like for Cole, Zuber, Ivey, and Kocamustafaogullary-Ishii’s correlations [6]. As such, the bubble departure frequency is exponentially proportional to the bubble departure diameter. Using Eq. (8), the bubble departure frequency can be written as follows:

$$f_b = c_f d_b^q = c_f (d_{b,0} \Delta T_{sat}^m)^q = f_{b,0} (T_w - T_{sat})^{qm} \tag{9}$$

where $f_{b,0} = c_f d_{b,0}^q$. In this study, we just attempt to examine the models/correlations of the heat flux partitioning, nucleation site density and bubble departure diameter. Hence, a detailed discussion on the bubble departure frequency correlations was not provided. For predicting the bubble departure frequency, only Cole’s correlation given bellow was used.

$$f_b = \sqrt{\frac{4g\Delta\rho}{3d_b\rho_l}} \tag{10}$$

2.5. Models Implementation

Substituting the nucleation site density, bubble departure diameter and bubble departure frequency given by Eqs. (7–9) into the heat flux partitioning model given by Eqs. (1–5), we have

- For $N_a = N_{a,0} (T_w - T_{sat})^n$,

$$F(T_w) = q_{q,0} (T_w - T_{sat})^{n+2m+qm/2} (T_w - T_l) + q_{e,0} (T_w - T_{sat})^{n+3m+qm} + h_c g(T_w) (T_w - T_l) - q_w = 0 \quad (11)$$

where

$$q_{q,0} = \left(\frac{4}{\pi} k_l \rho_l C_{pl} f_0 \right)^{1/2} A_{2f,0}$$

$$q_{e,0} = N_{a,0} f_0 \frac{\pi d_{b,0}^3}{6} \rho_v h_{fg}$$

$$A_{2f,0} = N_{a,0} \frac{\pi d_{b,0}^2}{4} K$$

- For $N_a = N_a (R_c(T_w))$,

$$F(T_w) = q_{q,0} N_a (T_w) (T_w - T_{sat})^{2m+qm/2} (T_w - T_l) + q_{e,0} N_a (T_w) (T_w - T_{sat})^{3m+qm} + h_c g(T_w) (T_w - T_l) - q_w = 0 \quad (12)$$

where

$$q_{q,0} = \left(\frac{4}{\pi} k_l \rho_l C_{pl} f_0 \right)^{1/2} A_{2f,0}$$

$$q_{e,0} = f_0 \frac{\pi d_{b,0}^3}{6} \rho_v h_{fg}$$

$$A_{2f,0} = N_{a,0} \frac{\pi d_{b,0}^2}{4} K$$

Note that $N_a(T_w) = N_a(R_c(T_w))$ and $g(T_w) = \max(1 - A_q, 0)$. Equations (11–12) are solved by using Newton-Raphson method, which employs the following iteration.

$$T_w^{k+1} = T_w^k - \frac{F(T_w^k)}{F'(T_w^k)} \quad (13)$$

This iteration will be convergent if $(T_w^{k+1} - T_w^k)/T_w^k < 10^{-4}$. By this way, a lot of models/correlations can be easily implemented into the computational codes.

3. PREDICTION OF DEBORA TESTS

In this section, several combinations of the selected wall boiling models were assessed against DEBORA experiment, which measured the subcooled forced convective boiling of refrigerant R-12 in a vertical tube having an inner diameter of 19.2 mm. The test section is sketched in Fig. 6. A detailed description of the DEBORA test facility can be found in Garnier et al. [17].

3.1. Experimental conditions

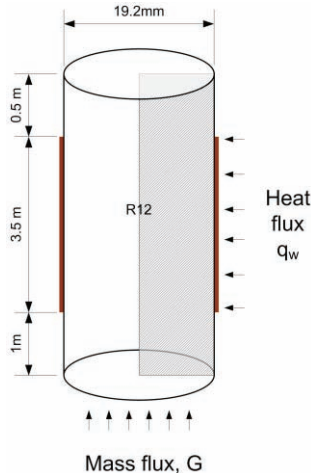


Figure 5. DEBORA Test Section

Two experimental tests of different pressures P and inlet liquid temperature T_{inlet} listed in Table III were investigated in this study. The relevant material properties of both liquid and vapor were taken from the National Institute of Standards and Technology (NIST) Standard Reference Database on Thermophysical Properties of Fluid Systems (<http://webbook.nist.gov/chemistry/fluid>).

Table III. Experimental Conditions

	P [MPa]	G [kg/m ² s]	q_w [kW/m ²]	T_{inlet} [°C]
Deb1	1.46	2029	76.24	34.9
Deb2	2.62	1985	73.89	70.5

3.2. Model Setup

The assessment was performed using a CFD code, namely EAGLE, which aims for multi-dimensional analyses of subcooled flow boiling. This CFD code uses the two-fluid model, which is beneficial to treat the behavior of each phase separately and to consider a phasic interaction term properly [18].

In the present simulation of the DEBORA experiment, four blocks of models were set up as follows:

- **Interfacial transfer models:** Ishii and Zuber's (1979) drag force, Tomiyama's (2002) lift force, Tomiyama's (1998) lubrication force, and Lahey et al.'s (1993) turbulent dispersion force
- **Turbulence models:** Standard k- ϵ model and Plegger-Becker's (2001) turbulent source terms
- **One-group IATE:** Yao and Morel's (2004) model
- **Wall boiling models:**
 - * *Heat flux partitioning:* Kural and Podowski's model with/without the micro-convection effect
 - * *Nucleation site density:* Lemmert and Chawla (LC) and Hibiki and Ishii (HI)'s correlations
 - * *Bubble departure diameter:* Fritz, Cole and Rohsenow (CR), Tolubinsky and Kostanchuk (TK), Kocamustafaogullari and Ishii (KI), and Unal's correlations
 - * *Bubble departure frequency:* Cole's correlation

3.3. Result and Discussion

At firstly an assessment of the bubble departure diameter correlations was presented. The correlations were combined with a widely used correlation of the nucleation site density, i.e. Lemmert and Chawla, and with original Kural and Podowski's model of the heat flux partitioning. As seen in Figs. 6–7, only LC-TK and LC-Unal combinations obtained a good prediction of the void fraction, IAC, and Sauter mean diameter for both the cases Deb1 and Deb2 while the others are underestimated. The radial profiles of these parameters predicted by the LC-TK and LC-Unal combinations closely match the experimental profiles measured at the outlet of the test section. The results strongly relate to the characteristics of the near-wall boiling heat transfer. It is clear that the larger bubble departure diameter and larger bubble departure frequency is the main reasons leading to the good prediction of the LC-TK and LC-Unal combinations. If the bubbles are too small and released with a low frequency, the void fraction, IAC and Sauter mean diameter are very small even with a large number of the bubbles generated. Although both Tolubinsky-Kostanchuk and Unal's correlations showed a good performance, Unal's correlation is more reasonable according to the assessment given above. It was, therefore, selected for the following assessments.

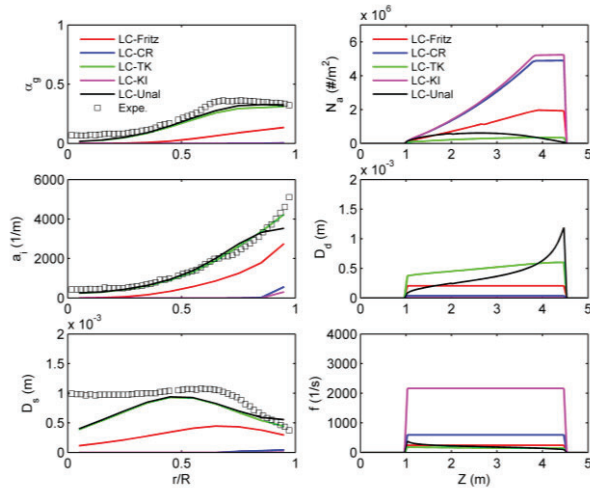


Figure 6. Bubble Departure Diameter (Deb1).

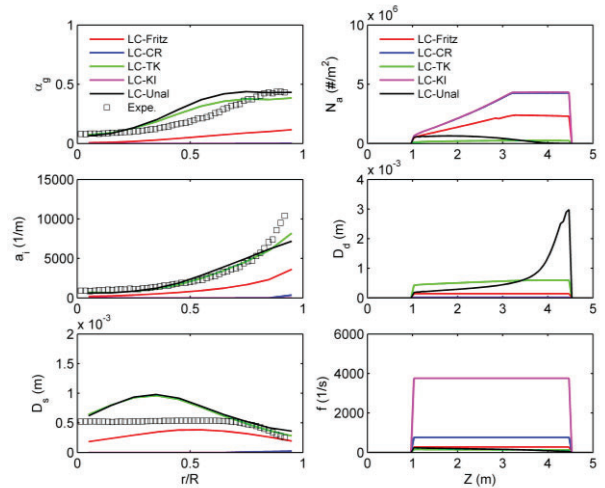


Figure 7. Bubble Departure Diameter (Deb2).

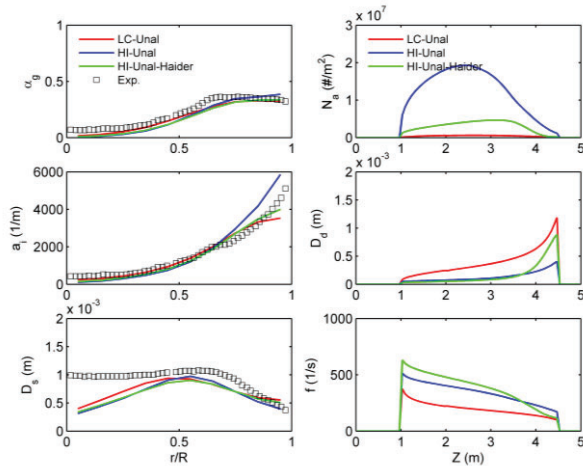


Figure 8. Nucleation Site Density (Deb1)

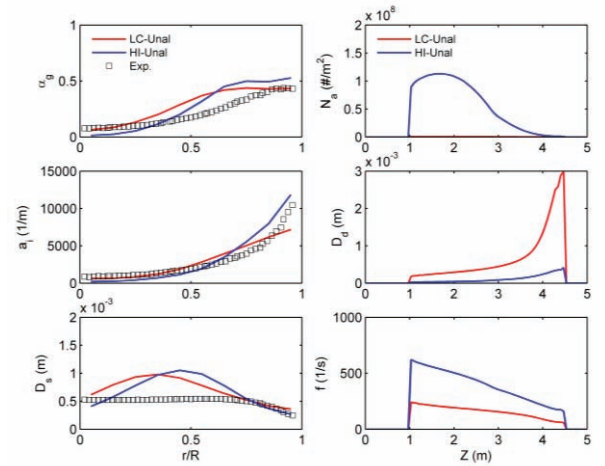


Figure 9. Nucleation Site Density (Deb2)

Sequentially, the nucleation site density correlations were taken into account. Two nucleation site density correlations, i.e. Lermmert-Chawla and Hibiki-Ishii's correlations which provided a good prediction for the published experimental data as presented in the Section 2.2, were compared. Unal's correlation for predicting the bubble diameter was selected to couple with these correlations. The other bubble departure diameter correlations were attempted to couple with HI's correlation, but the convergence criterion was not reached. As shown in Figs. 8–9, the radial profiles of the void fraction, IAC and Sauter mean diameter predicted by the LC-Unal and HI-Unal combinations closely match the experimental data profiles for both the cases. However, the nucleation site density predicted by Hibiki and Ishii's correlation is about three times as larger as that predicted by Lermmert and Chawla's correlation. This turns to reduce the bubble departure and bubble departure frequency to reach the agreement of the void fraction, IAC and Sauter mean diameter in the case of the HI-Unal combination.

In addition, the modified Kural and Podowski's heat flux partitioning model (denoted by 'Haider' in the HI-Unal-Haider combination) in which the micro-convection effect was integrated into the quenching component was compared, as shown in Fig. 8. An effort to couple the modified heat flux partitioning

model with the other correlations of the nucleation site density and bubble departure diameter was carried out, but only the HI-Unal combination is possible and this combination can predict only for the case Deb1. The results obtained with this combination also agree with the experimental data on the void fraction, IAC and Sauter mean diameter. The micro-convection effect just results in a significant reduce of the nucleation site density, as observed in Fig. 8.

The agreement of the void fraction, IAC and Sauter mean diameter as shown in above is frequently encountered in most CFD analyses of the subcooled boiling flows [2–6]. Nevertheless, the results seem physically unreasonable. The characteristics of the near-wall boiling heat transfer, i.e. the nucleation site density, bubble departure diameter and bubble departure frequency, predicted by the models/correlations are very different for the same problem. It is very possible that these characteristics varied according to the used model combinations to satisfy the energy balance at the heated surface, as given in Eq. (1). Indeed the evaporation, quenching and convection heat flow rates calculated varied significantly with the model combinations, as seen in Figs. (10–11). A general trend of these heat flow rates is that the convective component is dominant at the entrance of the heated region, then it turn to quenching component and finally to evaporation component. This trend is very natural. At the entrance region the subcooling effect is significant, hence lower wall temperature (smaller nucleation site density) and smaller bubble size. The convection heat transfer is therefore dominant in this region. Next to the middle region, more bubbles are generated and departure leading to narrow down the convective heat transfer area and enhance the quenching phenomenon. In contrast, at the outlet region much large bubbles are generated and prevent the subcooled liquid reaching to the heated surface. Thus, both the convective and quenching components reduced remarkably. Despite having the same trend, the components interchanged their magnitude so that the energy balance was reached.

Although Hibiki and Ishii’s correlation was showed to be a good correlation of the nucleation site density, the wall temperature predicted by the combination of this correlation with Unal’s correlation of the bubble departure diameter is too low, just about 3°C over the saturation temperature as seen in Figs. 12–13. Meanwhile, the wall temperature predicted by Lemmert and Chawla’s correlation coupling with Unal’s correlation seems reasonable. It is about 8°C as higher as the saturation temperature. This result raises a doubt that if both Hibiki-Ishii and Unal’s correlations are good enough as estimated above, which models/correlations are not appropriate? Perhaps, the problem lies in the heat transfer mechanisms by which the heat is taken away from the heated surface. As found recently, the evaporation of the microlayer under the bubble just accounts for less than 25% of the overall heat transfer while the large part is transferred via the evaporation of the superheated liquid surrounding the bubbles [19]. Possibly, the evaporation of the superheated liquid layer and also the condensation at the top of the bubbles take an important part in the heat transfer at the heated surface.

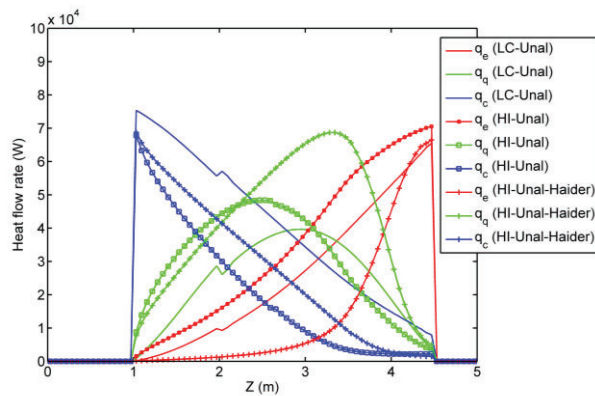


Figure 10. Heat Flux Partition (Deb1).

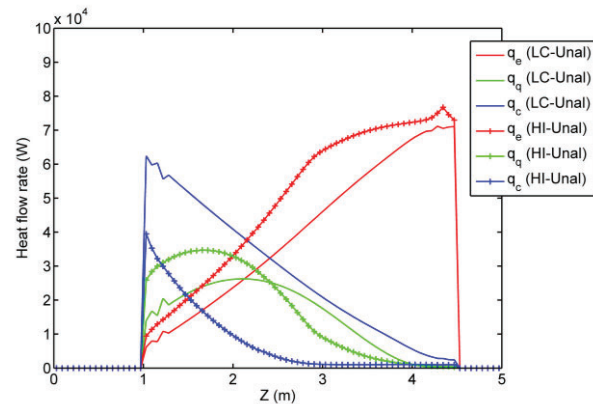


Figure 11. Heat Flux Partition (Deb2).

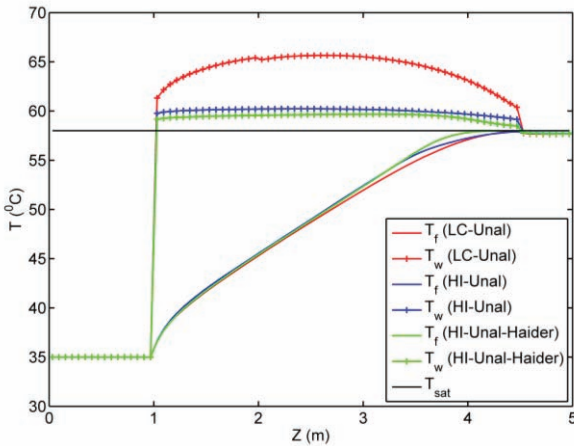


Figure 12. Liquid and Wall Temperatures (Deb1).

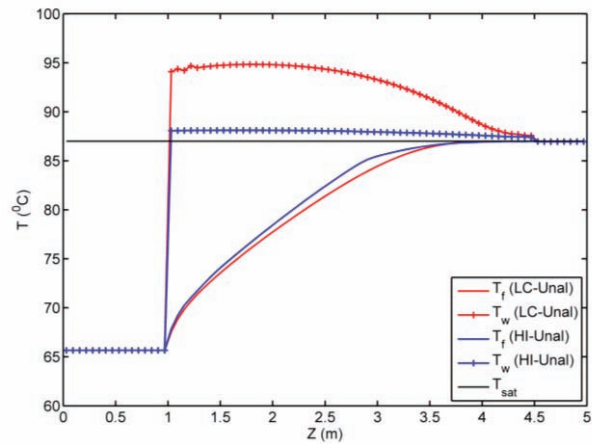


Figure 13. Liquid and Wall Temperatures (Deb2).

4. CONCLUSIONS

Numerous models and correlations for predicting the near-wall heat transfer in the subcooled flow boiling have been proposed. However, their applicability is very limited and debatable. On the heat flux partitioning, Kural and Podowski's model has been used widely in CFD simulations, but it does not account for the effects of the overlap of influential areas as well as the bubble sliding and bubble mergers. A model/correlation or at least a factor accounting for the effects is necessary. On the nucleation site density and bubble departure diameter, two correlations, i.e. Hibiki-Ishii and Unal's correlations, provide the best predictions for the published experimental data in comparison with the others. Nevertheless, when combining the separate models/correlations for the simulation of DEBORA experiment that investigated the forced convective subcooled boiling of refrigerant R-12 in a vertical tube, the results obtained seem unreasonable. The predicted boiling flow characteristics, i.e. void fraction, IAC and Sauter mean diameter, closely match the experimental data while the relevant near-wall boiling heat transfer characteristics, i.e. nucleation site density, bubble departure diameter, bubble departure frequency, divided heat flow rates and wall temperature, are significant different for the same problem. In fact, the near-wall boiling heat transfer characteristics were self-adjusted according to the used models/correlation to satisfy the energy balance at the heated surface. This means the used models/correlations did not reflect exactly the physical characteristics of the near-wall boiling heat transfer process. The problem possibly lies in the mechanisms by which the total heat flux is partitioned. The contribution of the heat transfer by means of the evaporation of superheated liquid surrounding the bubbles and by the condensation at the top of the bubbles to the total heat transfer can be significant and need to be accounted for.

ACKNOWLEDGMENTS

This work was supported by the National Research Foundation of Korea (NRF) grant funded by the Korea government (MISP) (No. 2012M2A8A4004176).

REFERENCES

1. V.K. Dhir, "Mechanistic Prediction of Nucleate Boiling Heat Transfer – Achievable or A Hopeless Task?," *J. Heat Transfer*, **128**, 1-12 (2005).
2. J.Y. Tu, G.H. Yeoh, "On Numerical Modeling of Low-Pressure Subcooled Boiling Flows," *Int. J. Heat Mass Transfer*, **45**, 1197-1209 (2002).

3. E. Krepper, R. Rzehak, "CFD for Subcooled Flow Boiling: Simulation of DEBORA Experiments," *Nucl. Eng. Design*, **241**, 3851-3866 (2011).
4. I.M. Asher, T.J. Drzewiecki, K.J. Fidkowski, T.J. Downar, "Parameter Sensitivity Study of Boiling and Two-Phase Flow Models in Computational Thermal Hydraulics," *NURETH-14*, Toronto, Canada, September 25-30, 2011 (2011).
5. B.J. Yun, A. Splawski, S. Lo, C.H. Song, "Prediction of A Subcooled Boiling Flow with Advanced Two-Phase Flow Models," *Nucl. Eng. Design*, **253**, 351-359 (2012).
6. S.C.P. Cheung, S. Vahaji, G.H. Yeoh, J.Y. Tu, "Modeling Subcooled Flow Boiling In Vertical Channels At Low Pressures – Part 1: Assessment of Empirical Correlations," *Int. J. Heat Mass Transfer*, **75**, 736-753 (2014).
7. G.R. Warrier, V.K. Dhir, "Heat Transfer and Wall Heat Flux Partitioning During Subcooled Flow Nucleate Boiling—A review," *J. Heat Transfer*, 128(12), 1243-1256 (2006).
8. S.I. Haider, R.L. Webb, "A Transient Micro-Convection Model of Nucleate Pool Boiling," *Int. J. Heat Mass Transfer*, **40**(15), 3675-3688 (1997).
9. V.H. Del Valle, D.B.R. Kenning, "Subcooled Flow Boiling At High Heat Flux," *Int. J. Heat Mass Transfer*, **28**(10), 1907-1920 (1985).
10. L.Z. Zeng, J.F. Klausner, "Nucleation Site Density in Forced Convection Boiling," *J. Heat Transfer*, **115**, 215-221 (1993).
11. T. Hibiki, M. Ishii, "Active Nucleation Site Density in Boiling Systems," *Int. J. Heat Mass Transfer*, **46**, 2587-2601 (2003).
12. J.F. Klausner, R. Mei, D.M. Berhad, L.Z. Zeng, "Vapor Bubble Departure in Forced Convection Boiling," *Int. J. Heat Mass Transfer*, **36**(3), 651-662 (1993).
13. R. Situ, T. Hibiki, M. Ishii, M. Mori, "Bubble Lift-Off Size in Forced Convective Subcooled Boiling Flow," *Int. J. Heat Mass Transfer*, **48**, 5536-5548 (2005).
14. W.G.J. Van Helden, C.W.M. Vander Geld, P.G.M. Boot, "Forced on Bubbles Growing and Detaching in Flow Along a Vertical Wall," *Int. J. Heat Mass Transfer*, **38**(11), 2075-2088 (1995).
15. V. Podanovic, D. Fraser, M. Salcudean, "Bubble Behavior in Subcooled Flow Boiling of Water at Low Pressure and Low Flow Rates," *Int. J. Multiphase Flow*, **28**, 1-19 (2002).
16. I.C. Chu, "Application of Visualization Techniques to the Boiling Structures of Subcooled Boiling Flow and Critical Heat Flux," *KAIST PhD. Thesis*, Deajeon, Korea (2011).
17. J. Garnier, E. Manon, G. Cubizolles, "Local Measurement on the Flow Boiling of Refrigerant 12 in a Vertical Tube," *Multiphase Sci. Technol.*, **13**, 1-111 (2011).
18. B.U. Bae, B.J. Yun, H.J. Yun, D.J. Euh, C.H. Song, "Development of CFD Code for Subcooled Boiling Two-Phase Flow with Modeling of the Interfacial Area Transport Equation," *KAERI report*, Deajeon, Korea (2008).
19. J. Kim, "Review of nucleate pool boiling bubble heat transfer mechanisms," *Int. J. Multiphase Flow*, **35**, 1067-1076 (2009).